Removal of early senescent cells protects retinal ganglion cells loss in experimental ocular hypertension.

Lorena Raquel Rocha[1±], Viet Anh Nguyen Huu[1±], Claudia Palomino La Torre[1], Qianlan Xu[1], Mary Jabari[1], Michal Krawczyk[1], Robert N. Weinreb[1], Dorota Skowronska-Krawczyk* [1, 2]

[1] Shiley Eye Institute, Hamilton Glaucoma Center and Viterbi Family Department of Ophthalmology, University of California, San Diego, 9500 Gilman Drive, La Jolla, California 92093, USA.

[2] Richard C. Atkinson Lab for Regenerative Ophthalmology, University of California, San Diego, 9500 Gilman Drive, La Jolla, California 92093, USA.

[±]equally contributed

*corresponding author

DorotaSK@ucsd.edu

Abstract

Experimental ocular hypertension induces senescence of retinal ganglion cells (RGCs) that mimicks events occurring in human glaucoma. Senescence-related chromatin remodeling leads to profound transcriptional changes including the upregulation of a subset of genes that encode multiple proteins collectively referred to as the senescence-associated secretory phenotype (SASP). Emerging evidence suggests that the presence of these proinflammatory and matrix-degrading molecules has deleterious effects in a variety of tissues. In the current study, we demonstrated in a transgenic mouse model that early removal of senescent cells induced upon elevated intraocular pressure (IOP) protects unaffected RGCs from senescence and apoptosis. Visual evoked potential (VEP) analysis demonstrated that remaining RGCs are functional and that the treatment protected visual function. Finally, a senolytic drug was used to remove endogenous senescent retinal cells upon IOP elevation and prevented loss on retinal function and structure. In sum, these studies suggest senolytic drugs as a potential new treatment in mitigation of the deleterious impact of high IOP on RGCs survival.

Introduction

The glaucomas are a group of progressive optic neuropathies characterized by degeneration of retinal ganglion cells and resulting changes in the optic nerve. It is a complex disease where multiple genetic and environmental factors interact[1,2]. Two of the leading risk factors, increased intraocular pressure (IOP) and age, are related to the extent and rate of RGC loss. Although lowering IOP is the only approved and effective treatment for slowing worsening of vision, many treated glaucoma patients continue to experience loss of vision and some become blind. Several findings suggest that age-related tissue changes themselves contribute significantly to the neurodegenerative changes that cause loss of vision. However, the specific molecular processes damaging the retinal ganglion cells (RGCs) in the aging eye are poorly understood.

In a mouse model of glaucoma/ischemic stress, we reported the effects of *p16Ink4a* on RGC death[2]. Upon increased intraocular pressure (IOP), the expression of *p16Ink4a* was elevated, leading to enhanced senescence in RGCs; this is what most likely directly causes loss of vision and further RGC death. In addition, the analysis of p16KO mice suggested that the lack of the *p16Ink4a* gene protected RGCs from cell death caused by elevated IOP[2]. Importantly, the elevated expression of *p16INK4a* and senescence were both detected in human glaucomatous eyes[2]. Therefore, for the first time, *p16Ink4a* was implicated as a downstream integrator of diverse signals causing RGC aging and death that are characteristics of the pathogenesis of glaucoma. Our findings were further supported by a subsequent report showing that *p16Ink4a* was upregulated by TBK1 activity and that this causes RGC death in ischemic retina injury [3]. It is also notable that a recent bioinformatic meta-analysis of a published set of genes associated with POAG

pointed at senescence and inflammation as key factors in RGC degeneration in glaucoma[4].

Glaucoma remains relatively asymptomatic until it is severe, and the number of affected individuals is much higher than the number diagnosed. Medeiros et al[5] examined and modeled the relationship between decreasing numbers of RGCs and first reports of the changes in vision. They estimated that up to about 28% of RGCs can be lost before any visual defects are detected. Numerous clinical studies have shown that lowering IOP slows the disease progression[6,7]. However, glaucoma damage is not halted but instead continues to worsen in most individuals. This suggests that there is a mechanism that continues to damage the optic nerve even after lowering the pressure.

The current investigation was undertaken to determine whether early removal of senescent RGCs that secrete senescent associated secretory proteins (SASP) will protect remaining RGCs from senescence and death induced upon IOP elevation in the eye. We now have used an established transgenic p16-3MR mouse model[8] in which the systemic administration of small molecule ganciclovir (GCV) selectively kills *p16INK4a*-expressing cells. Using this model, we show that the early removal of *p16Ink4*$^{+}$ cells has a strong protective effect on RGC survival and visual function. We confirm the efficiency of the method by showing the reduced level of *p16INK4a* expression and lower number of senescent β-galactosidase positive cells after the GCV treatment. Finally, we show that treatment of p16-3MR mice with an established senolytic drug has a similar protective effect on RGCs as GCV treatment. These data suggest the potential application of senolytic drugs to mitigate the deleterious impact of high IOP on RGCs.

MATERIALS AND METHODS

Animals

All animal experiments were approved by the UC San Diego Institutional Animal Care and Use Committee (IACUC) and adhered to the ARVO Statement for the Use of Animals in Ophthalmic and Vision Research. Adult p16-3MR[8] or C57BL/6 mice (12-16 weeks old, Jackson Labs) were housed in 20 ºC environment with standard (12 h light/dark) cycling, food and water available ad libitum. For all experiments, an equal number of male and female mice were used.

Drug treatment

The p16-3MR transgenic model (**Figure 1A**), in which the mice carry a trimodal reporter protein (3MR) under the control of p16 regulatory region[8] , allows potent selective removal of senescent cells. The 3MR transgene encodes a fusion protein consisting of Renilla luciferase, a monomeric red fluorescent protein (mRFP) and herpes simplex virus thymidine kinase (HSV-TK) which converts ganciclovir (GCV) into a toxic DNA chain terminator to selectively kill HSV-TK expressing cells. The experimental group of animals was treated by intraperitoneal (IP) administration of GCV (Sigma, 25mg/kg once a day) or dasatinib (Sigma, 5mg/kg) after IOP elevation (see below), and a control group of mice was sham-treated with PBS or vehicle (DMSO). Each mouse underwent unilateral hydrostatic pressure-induced IOP elevation to 90 mm Hg, with the contralateral eye left as an untreated control. The mice were IP injected with GCV or dasatinib at day 0 (IOP elevation day) and continued for four consecutive days (**Figure 1B**). At day 5, animals were euthanized, retinas were isolated and immunostained with anti-Brn3a antibody to evaluate the number of RGCs. All drugs were prepared according to the UC San Diego

Institutional Animal Care and Use Committee (IACUC) standards. To ensure a sterile environment, this compound is prepared under the tissue culture hood and sterile PBS is used. The final solution is filtered through a 0.22um PES membrane just before injection. Tips, tubes, and syringes involved in the preparation of the compound are sterile.

Hydrostatic intraocular pressure (IOP) elevation

Animals were anesthetized with an intraperitoneal injection of ketamine/xylazine cocktail, (100 mg/kg and 10 mg/kg, respectively), their eyes anesthetized with one drop of proparacaine (0.5 %, Bausch-Lomb) and dilated with one drop of tropicamide (1 %, Alcon Laboratories). Unilateral elevation of IOP was achieved by infusing Balanced Salt Solution (Alcon Laboratories) into the anterior chamber of the eye through an IV infusion set. The level of IOP increase was determined by the height of the saline bottles on the IV infusion set. Stable elevated IOP of 85-90mm Hg was maintained for 60 minutes, and controlled by IOP measurements using a veterinary rebound tonometer (Tonovet). Both eyes were lubricated throughout testing with an ophthalmic lubricant gel (GenTeal, Alcon Laboratories). Animals recovered on a Deltaphase isothermal pad (Braintree Scientific) until awake. The contralateral eye without IOP elevation served as a healthy non-IOP control (CTRL).

Visual evoked potential (VEP)

VEP measurements were taken at five days post-IOP elevation. This protocol was adapted from prior studies[9]. Mice were dark adapted for at least 12 hours before the procedure. Animals were anesthetized with ketamine/xylazine as mentioned earlier, and their eyes dilated as previously mentioned. The top of the mouse's head was cleaned with an antiseptic solution. A scalpel was used to incise the scalp skin, and a metal

electrode was inserted into the primary visual cortex through the skull, 0.8 mm deep from the cranial surface, 2.3 mm lateral to the lambda. A platinum subdermal needle (Grass Telefactor) was inserted through the animal's mouth as a reference, and through the tail as ground. The measurements commenced when the baseline waveform became stable, 10-15 s after attaching the electrodes. Flashes of light at 2 log cd.s/m^2 were delivered through a full-field Ganzfeld bowl at 2 Hz. Signal was amplified, digitally processed by the software (Veris Instruments), then exported and peak-to-peak responses were analyzed in Excel (Microsoft). To isolate VEP of the measured eye from the crossed signal originating in the contralateral eye, a black aluminum foil eyepatch was placed over the eye not undergoing measurement. For each eye, peak-to-peak response amplitude of the major component N1 in IOP eyes was compared to that of their contralateral NIOP controls. Following the readings, the animals were euthanized, and their eyes collected and processed for immunohistological analysis.

Immunohistochemistry

Following euthanisa, their eyes were enucleated and fixed in 4% paraformaldehyde (PFA) in PBS (Affymetrix) for 1 hour and subsequently transferred to PBS. The eyes then were dissected, the retinas flat-mounted on microscope slides, and immunostained using a standard sandwich assay with anti-Brn3a antibodies (Millipore, MAB1595) and secondary AlexaFluor 555 Anti-mouse (Invitrogen, A32727). Mounted samples (Fluoromount, Southern Biotech 0100-01) were imaged in the fluorescent microscope at 20x magnification (Biorevo BZ-X700, Keyence), focusing on the central retina surrounding the optic nerve. Overall damage and retina morphology were also taken into consideration for optimal assessment of general effect. Micrographs were quantified using

manufacturer software for Brn3a-positive cells in 6 independent 350 μm x 350 μm areas per flat-mount.

Real-Time PCR

Total RNA extraction from mouse tissues, cDNA synthesis, and RT-qPCR experiments were performed as previously described[2]. Assays were performed in triplicate. Relative mRNA levels were calculated by normalizing results using GAPDH. The primers used for RT-qPCR are listed in Table S2. The differences in quantitative PCR data were analyzed with an independent two-sample t-test.

SA-βgal Assay to Test Senescence on Retinas Mouse Eyes

Senescence assays were performed using the Senescence b-Galactosidase Staining Kit (Cell Signaling) according to the manufacturer's protocol. Images were acquired using a Hamamatsu Nanozoomer 2.0HT Slide Scanner and quantified in independent images of 0.1 mm^2 covering the areas of interest using Keyence software.

RNA-Seq analysis

High-quality RNAs were extracted using TRIzol Reagent (Invitrogen) and treated with TURBO DNA-free Kit (Invitrogen). RNA-Seq libraries were made from 1 μg total RNA per tissue sample using TruSeq stranded mRNA Library Prep Kit (Illumina, kit cat. no. 20020597) according to the manufacturer's instructions. The libraries were subjected to size selection using Agencourt Ampure XP beads (Beckman Coulter) and quality checked by Tape Station (Agilent). Strand-specific RNA-Seq paired-end reads sequence data (PE50: 2×50 bp) were obtained using HiSeq4000 system. Raw reads were mapped using Tophat/Bowtie2 with –very-sensitive parameters[10]. Read

counting, normalization and identification of differentially expressed genes was done using Cufflinks package[11]. Expression heatmaps were generated using online tool Morpheus maintained at https://software.broadinstitute.org/morpheus/. Gene ontology analyses of the sets of differentially expressed genes was performed using PANTHER[12]

RESULTS

Intraocular pressure was increased in one eye of transgenic mice bearing p16-3MR construct (**Figure 1A**). After IOP elevation mice were intraperatenoaly treated with GCV for five consecutive days (**Figure 1B)** to specifically deplete p16^{+} cells**.** In parallel, wild-type animals were subjected to the same protocol, i.e., underwent five GCV daily injections after unilateral IOP elevation. Using flat mount immunohistochemistry and retinal ganglion cell quantification we observed that five-day administration of GCV after IOP elevation had a significant protective effect on Brn3a^{+} RGC number in p16-3MR mice when compared to untreated eye (**Figure 1C, D**) but not in WT animals (**Figure 1E**) suggesting that the effect of the GCV injection is specific to the mice harboring the transgene.

Next, to test whether the protection of cell number in the GCV treated retinas is accompanied by the protection of the the visual circuit integrity on day five, the *in vivo* signal transmission from the retina to the primary visual cortex was measured using visual evoked potentials (VEP) (**Figure 2A**)[13,14]. Using this approach, we have found that eyes subjected to IOP elevation have decreased VEP P1-N1 amplitude (**Figure 2B**), compared to contralateral non-IOP control eyes. However, there was a marked rescue of VEP signals in transgenic animals treated with a small molecule (**Figure 2B).** Further quantification showed significant vision rescue upon GCV treatment only in p16-3MR and not WT animals (**Figure 2C, D**); this suggested that the GCV treatment can have only protective effect on structure and function of the retina in transgenic animals.

Our previous studies indicated that the *p16INK4a* elevated expression could be first observed as early as day three post-IOP elevation[2]. Therefore, we chose day three post-

IOP to analyze the effectiveness of the treatment on early senescent cells. RGC quantification showed that in animals not injected with GCV only ~15-20% of cells disappeared at day 3 (compared to ~45-50% on day 5). Interestingly, this number is not significantly changed in retinas isolated from GCV treated animals (**Figure 3A).** This shows that as early as at day three, a small portion of cells already has undergone cell death upon IOP elevation. Additionally, these data suggest that most of the senescent cells in the five days GCV treatment experiment are removed already at day three since the levels are comparable to these observed at day five in p16-3MR treated animals (**Figure 1C, D)**.

To test whether our treatment indeed removed the presence of senescent cells in the retina we used two approaches. First, we quantified the *p16Ink4a* expression at day three post-treatment and observed the striking loss of expression of the gene in IOP retinas upon GCV treatment (**Figure 3B**). Second, we further confirmed this notion by performing the senescence-associated β-galactosidase assay and observed a significant decrease in a number of senescent cells at day three post-IOP in the GCV treated animals (**Figure 3C, D**).

Next, to understand the changes undergoing in the retina at the molecular level, we wanted to investigate the transcriptional effect of IOP elevation and GCV treatment. To select the day when RGCs are still present but undergoe the highest level of changes we performed time-course experiment to follow the activation of caspase as a marker of endogenous stress in the cell (**Figure 4A** *left*). After quantification, we have noted that the highest level of RGCs labelled with activated caspase antibody is at day 3 after IOP elevation (**Figure 4A** *right*). Interestingly, at this time point there is still most of the RGCs

present in the tissue. This stage also corresponds to the highest expression of senescence associated factors as previously noted[2]. Therefore we chose this time point for our molecular analysis. RNA-seq analysis was performed on total RNA isolated from 3 retinas in each experimental group. Of the total 21351 detected gene loci, 1601 were significantly de-regulated by the IOP treatment; 999 detected gene loci were up-regulated and 602 down-regulated (**Figure 4B**, ***top***). When the IOP treatment was performed in mice treated with GCV, the total numbers of IOP-affected genes changed modestly to 1707, with 848 up-regulated and 859 down-regulated (**Figure 4B**, ***bottom***).

To inquire in an unbiased way about the differences in signaling pathways and cellular processes affected by IOP, GO analysis using PANTHER was performed[12]. This approach revealed that processes of the immune system response, inflammation, and extracellular matrix composition and cell-matrix interaction were significantly changed in IOP samples (**Table 1**). We have also detected the significantly deregulated genes involved in apoptosis, microglial activation and interlukin-6 and 8 production and secretion. This analysis shows that many mechanisms are induced upon an acute IOP elevation, most probably causing additional transcriptional stress to cell.

Further analysis revealed that the genes involved in cellular senescence, extracellular matrix molecules and in factors involved in apoptosis (**Table 2**)[15] were significantly de-regulated upon IOP elevation. Importantly, 3-day treatment to remove p16+ cells significantly mitigated this response (**Figure 4C**). This data is in agreement with the loss of the senescence cells upon GCV treatment (**Figure 3B, C, D**) and lower detrimental impact of senescent cells on surrounding cells.

Finally, a list of 617 genes was used which were significantly de-regulated upon increase of IOP (**Figure 4D)** , specifically in retinas not treated with GCV. The GO analysis of this subset of genes identified a specific enrichment of a class of genes belonging to the ABL1 pathway and ABL1 downstream targets (**Fig S1**), suggesting that IOP treatment de-regulated the ABL1 pathway in senescing cells. As a result, we explored whether the well defined senolytic drug dasatinib, a Bcr-Abl and Src family threonine kinase inhibitor, could have a beneficial effect similar to GCV in p16-3MR mice. To test the protective effect of dasatinib in the retina after IOP elevation, mice were treated with dasatinib (5mg/kg) or vehicle for 5 days. We followed the experimental procedure used for GCV treatment (**Figure 1B**) in p16-3MR mice to compare the efficiency of both treatments in the same mice strain. At day five after IOP elevation, VEP measurement was performed and retinas were immunostained to quantify RGC loss. Upon this treatment, we noticed that there was no significant loss of cells in retinas isolated from dasatinib treated mice (**Figure 5C**) similar to what was observed in GCV treated animals (**Figure 1E**). Most importantly, VEP analysis revealed that senolytic drug treatment successfully prevented vision loss upon IOP elevation (**Figure 5D**).

DISCUSSION

P16INK4a expression and accumulation of senescent cells in the glaucomatous retina have been previously associated with RGC death[2,3]. Here, we show that in transgenic animals that have expression of viral TK under the control of regulatory regions of p16Ink4a[8] ,selective removal of early senescent cells is beneficial for remaining cells in the retinal tissue undergoing stress upon IOP elevation. In this model, the presence of GCV is selectively inducing death of transgene-expressing cells. By starting GCV

application as soon as day 0 after the IOP elevation and continued for five consecutive days, early removal of *p16Ink4a* expressing cells protects neighboring RGCs from death. Using VEP, cells remaining in the tissue after GCV treatment are still able to provide a signal to the visual cortex, therefore demonstrating that protected cells are still functional.

Upon GCV injection, we also show that there are fewer senescent cells present at day three of treatment and that the transcriptional program of cells is changed as compared to retinas from untreated mice. In particular, we note significant changes in the senescence program as well as in the extracellular matrix (ECM) function. Moreover, the both pathways are downregulated by GCV treatment. Finally, we show that dasatinib, a known senolytic drug, can be used to protect RGCs from death, further confirming that early removal of senescent cells induced upon IOP elevation protects retina health.

Taken together, we propose a model (**Figure 5E**) where early damaged cells become senescent and start to express SASP molecules upon elevated IOP. During disease progression, SASP molecules induce apoptosis and senescence in neighboring cells. RGC apoptosis causes loss of axons and optic nerve degeneration. When early senescent cells are removed using the drug (**Figure 5E, *bottom***), the neighboring cells are not exposed to detrimental SASPs, and the disease progression is significantly slowed down. The remaining cells are healthy.

We and others previously used 90 mm Hg as an extremely acute and reproducible way to induce cell response and RGC death[2]. However, this level of pressure is likely an ischemic insult. The resulting synchronized and quick cell death provide unique qualities that are extremely useful for molecular and biochemical studies, however they are not fully representative of primary open angle glaucoma, a chronic optic neuropathy.

However, this acute insult allows study of the time course of stress response and can help unravel important aspects of stepwise response of cells to elevated intraocular pressure.

Lowering IOP is the only approved and effective glaucoma treatment. Results from many clinical trials indicated that decreasing intraocular pressure can prevent and slow disease progression[1]. However, many glaucoma patients who have received the treatment continue to experience deterioration of visual acuity and a slow progression towards blindness. Similarly, it has been noted that some patients with an acute elevaion of intraocular pressure have delayed functional vision loss despite the surgical intervention to normalize the intraocular pressure[16,17]. Altogether, this suggests that some initial changes in the retina induced by acute or chronic IOP changes continue to affect the tissue even after the lowering IOP.

Mammalian aging is a complex process where distinct molecular processes contribute to age-related tissue dysfunction. While no single defect defines aging, several lines of evidence suggest that activation of senescence is a vital contributor[18]. Cellular senescence has been conventionally viewed as an irreversible cell-cycle arrest mechanism, but multiple recent findings have extended its role to complex biological processes such as development, tissue repair, aging, and age-related disorders. Emerging evidence suggests that a major drawback of senescence is the prolonged presence of the proinflammatory and matrix-degrading molecules (SASPs) in the tissue. Markers of cellular senescence such as expression of the *p16Ink4a* and SASP molecules dramatically increase during aging in both humans and mice. Several studies suggest that *p16Ink4a*+ cells act to shorten healthy lifespan by promoting age-dependent changes

that functionally impair tissues and organs[19-22]. Intriguingly, a recent explosion of studies has shown that removal of senescent cells using senolytic drugs in progeroid (accelerated aging phenotype) and healthy mice induces lifespan extension and improves the health of animals[19,23-25]. Our work shows for the first time that using a similar approach we can protect the death of RGCs caused by senescence, induced upon IOP elevation.

Dasatinib is the is a selective tyrosine kinase receptor inhibitor that is commonly used in the therapy of chronic myelogenous leukemia (CML). Other studies have shown that treatment with dasatinib is effective in destroying senescent fat cells[26]. Our RNA-seq data suggested this senolytic drug as a first candidate for the treatment upon IOP elevation. Notably, we found that the level of RGC protection resembles the one obtained with the GCV treatment. Based on these findings, we conclude that dasatinib removed senescent cells, and consequently protected the remaining RGCs in p16-3MR mice retinas. Our p study of the possible therapeutic effects of dasatinib suggests further study of senolytic drug effects on the eye.

The gene encoding *p16INK4a*, *CDKN2A*, lies within the INK4/ARF tumor suppressor locus on human chromosome 9p21; this is the most significant region to be identified as having an association with POAG in different population samples[27]. *CDKN2A* encodes two transcripts with alternative transcriptional start sites - *p16INK4a* and *ARF* (*p14ARF* in humans and *p19Arf* in mice). In addition to *CDKN2A*, the INK4/ARF locus encodes a third tumor suppressor protein, *p15INK4b*. A fourth INK4/ARF transcript, *ANRIL* (Antisense Noncoding RNA in the INK4/ARF Locus), is proposed to function as an epigenetic regulator of *INK4/ARF* gene transcription, targeting histone-modifying enzymes to the locus. Several collaborative efforts identified numerous SNPs localized within the 9p21

locus to be highly associated with the risk of open-angle glaucoma including Normal-Tension Glaucoma (NTG), a glaucomatous optic neuropathy not associated with elevated IOP[28,29]. Intriguingly, one of the top variants associated with risk of NTG is located in the gene TBK1, a factor that has been recently shown to be implicated in upregulation of *p16ink4a* gene[3]. Finally, recent studies have also revealed that specific methylation patterns in the 9p21 locus are strongly associated with the risk of NTG glaucoma[30]. It is notable that the positions of most, if not all, of these SNPs and methylation markers, overlap with active regulatory regions in the locus identified by ENCODE[31]. Although regulation of expression of genes within the 9p21 locus in many diseases and aging is under extensive investigation, it still needs to be explicitly investigated in relation to glaucoma.

Another major type of glaucomatous optic neuropathy is angle closure glaucoma (ACG), a condition characterized by blockage of the drainage angle of the eye. To date, there is no study reporting genetic variants or methylation markers in the 9p21 locus significantly associated with the risk of ACG while several studies implicated several molecular mechanisms of the disease[32]. Nevertheless, the progressive vision loss is found in PACG patients, even after lowering the IOP[16], raises the question whether such a relationship can be seen when studying the genetic variants correlating with the progression instead of the risk of the disease. Further studies to unravel whether such an association exists are needed.

Senolytic therapies have been applied in animal research to delay, prevent or alleviate multiple age-related phenotypes, chronic diseases, and geriatric syndromes[19,23-25]. Senolytic agents are being tested in clinical trials especially to target fundamental aging

mechanisms[33]. Our studies suggest a potential use of such therapy to reduce glaucoma blindness either as a sole treatment or as a complementary one with IOP-lowering therapies.

FIGURE LEGENDS

Figure 1. Removal of early senescent cells has a neuroprotective effect on RGCs. **A.** Schematic representation of the p16-3MR transgene. Triple fusion of luciferase, the red fluorescent protein and tyrosine kinase from HSV virus are under control of the regulatory region of p16Ink4a gene. **B.** Plan of the experiment. After unilateral IOP elevation mice are daily injected with GCV (25 mg/kg) intraperitoneally. At day 5 VEP is measured, and tissue is collected for further experiments. **C.** Representative images of retina flat mount immunohistochemistry at day five with anti-Brn3a antibody specifically labeling ~80% of RGC cells. **D.** Quantification of RGC number at day five after the treatment of WT animals. N=6 animals in each group **E.** Quantification of RGC number at day five after the treatment of p163MR animals. N=6 animals in each group. A statistical test was performed using ANOVA. * $p<0.05$, ** $p<0.01$, n.s. – not significant

Figure 2. Visual functions are preserved in animals when the early senescent cells were removed. **A.** Schematic representation of the placement of electrodes for VEP measurements. **B.** Example results of VEP experiments. Top: results of the VEP response of healthy and IOP treated eyes. Bottom: After GCV injections the VEP response is protected. **C.** Quantification of VEP responses at day five after the treatment of WT animals. **D.** Quantification of VEP responses at day 5 after the treatment of the p16-3MR animals N=6 animals; t-test, **$p<0.01$

Figure 3. Senescence is lowered upon GCV treatment. **A.** At day three after IOP, only 20% of RGCs is lost compared to the non-treated eye. GCV treatment is removing the same number of cells. n=4 (non-GCV) and n=6 (GCV), ANOVA, *$p<0.05$, **$p<0.01$, n.s. – not significant; **B.** p16Ink4a expression is significantly lower in affected retinas isolated from GCV treated p16-3MR animals at day three after IOP elevation. ttest, **$p<0.01$ **C.** Number of SA-b-gal positive cells is lowered upon GCV treatment. Blue arrow – remaining senescent cell; **D.** Quantification of a number of senescent cells upon IOP elevation in retinas isolated from mice treated and non-treated with GCV. n=8 animals; t-test, **$p<0.01$

Figure 4. Analysis of pathways affected in IOP treated retinas. **A.** Immunohistochemistry of Brn3a and activated caspase show an increase of apoptosis at day three after IOP treatment. **B.** RNA-seq analysis of the response to IOP and GCV. Eyes subjected to IOP elevation show a significant change in gene expression with genes equally upregulated and downregulated **C.** Heatmap analysis of genes involved in senescence, active oxidative species (ROS), apoptosis, extracellular matrix (ECM) and inflammation.

Figure 5. Dasatinib protects retina degeneration. A. plan of the experiment. After unilateral IOP elevation mice are daily injected with dasatinib (5 mg/kg) intraperitoneally. At day 5 VEP is measured, and tissue is collected for further experiments. Immunohistochemistry of Brn3a and activated caspase show an increase of apoptosis at day three after IOP treatment. **B.** Retina flat mount immunohistochemistry at day 5 with anti-Brin3a antibody specifically labeling ~80% of RGC cells. **C.** Quantification of RGC number at day five after the treatment of p16-3MR animals with dasatinib. N=6 animals in each group; **D.** Quantification of VEP responses at day five after the treatment of p16-3MR animals with dasatinib. **E.** Model. Top: Upon elevated IOP early damaged cells become senescent and start to express SASP molecules. While disease progresses, the SASP molecules induce senescence in neighboring cells. Prolonged senescence is causing RGCs death. Bottom: When early senescent cells are removed using senolytic drug the neighboring cells are not exposed to detrimental SASPs, and the disease progression is significantly slowed down. Remaining cells are healthy.

ACKNOWLEDGEMENTS

Research in DSK lab is supported in part by NIH R01 EY027011, Glaucoma Research Foundation Award, Research to Prevent Blindness Special Scholar Award and NIHCore Grant for Vision Research (P30EY022589).

REFERENCES

1 Weinreb, R. N., Aung, T. & Medeiros, F. A. The pathophysiology and treatment of glaucoma: a review. *JAMA* **311**, 1901-1911, doi:10.1001/jama.2014.3192 (2014).

2 Skowronska-Krawczyk, D. *et al.* P16INK4a Upregulation Mediated by SIX6 Defines Retinal Ganglion Cell Pathogenesis in Glaucoma. *Mol Cell*, doi:10.1016/j.molcel.2015.07.027 (2015).

3 Li, L. U., Zhao, Y. & Zhang, H. P16INK4a upregulation mediated by TBK1 induces retinal ganglion cell senescence in ischemic injury. *Cell Death Dis* **8**, e2752, doi:10.1038/cddis.2017.169 (2017).

4 Danford, I. D. *et al.* Characterizing the "POAGome": A bioinformatics-driven approach to primary open-angle glaucoma. *Prog Retin Eye Res* **58**, 89-114, doi:10.1016/j.preteyeres.2017.02.001 (2017).

5 Medeiros, F. A. *et al.* A combined index of structure and function for staging glaucomatous damage. *Arch Ophthalmol* **130**, 1107-1116, doi:10.1001/archophthalmol.2012.827 (2012).

6 Boland, M. V. *et al.* Comparative effectiveness of treatments for open-angle glaucoma: a systematic review for the U.S. Preventive Services Task Force. *Ann Intern Med* **158**, 271-279, doi:10.7326/0003-4819-158-4-201302190-00008 (2013).

7 Sihota, R., Angmo, D., Ramaswamy, D. & Dada, T. Simplifying "target" intraocular pressure for different stages of primary open-angle glaucoma and primary angle-closure glaucoma. *Indian J Ophthalmol* **66**, 495-505, doi:10.4103/ijo.IJO_1130_17 (2018).

8 Demaria, M. *et al.* An essential role for senescent cells in optimal wound healing through secretion of PDGF-AA. *Dev Cell* **31**, 722-733, doi:10.1016/j.devcel.2014.11.012 (2014).

9 Ridder, W. H. & Nusinowitz, S. The visual evoked potential in the mouse - Origins and response characteristics. *Vision Res* **46**, 902-913, doi:10.1016/j.visres.2005.09.006 (2006).

10 Kim, D. *et al.* TopHat2: accurate alignment of transcriptomes in the presence of insertions, deletions and gene fusions. *Genome Biol* **14**, R36, doi:10.1186/gb-2013-14-4-r36 (2013).

11 Trapnell, C. *et al.* Differential gene and transcript expression analysis of RNA-seq experiments with TopHat and Cufflinks. *Nat Protoc* **7**, 562-578, doi:10.1038/nprot.2012.016 (2012).

12 Mi, H., Muruganujan, A., Ebert, D., Huang, X. & Thomas, P. D. PANTHER version 14: more genomes, a new PANTHER GO-slim and improvements in enrichment analysis tools. *Nucleic Acids Res* **47**, D419-D426, doi:10.1093/nar/gky1038 (2019).

13 Bui, B. V. & Fortune, B. Ganglion cell contributions to the rat full-field electroretinogram. *J Physiol* **555**, 153-173, doi:10.1113/jphysiol.2003.052738 (2004).

14 Porciatti, V. Electrophysiological assessment of retinal ganglion cell function. *Exp Eye Res* **141**, 164-170, doi:10.1016/j.exer.2015.05.008 (2015).

15 Pawlikowski, J. S. *et al.* Wnt signaling potentiates nevogenesis. *Proc Natl Acad Sci U S A* **110**, 16009-16014, doi:10.1073/pnas.1303491110 (2013).

16 Brubaker, R. F. Delayed functional loss in glaucoma. LII Edward Jackson Memorial Lecture. *Am J Ophthalmol* **121**, 473-483 (1996).

17 Calkins, D. J. Critical pathogenic events underlying progression of neurodegeneration in glaucoma. *Prog Retin Eye Res* **31**, 702-719, doi:10.1016/j.preteyeres.2012.07.001 (2012).

18 He, S. & Sharpless, N. E. Senescence in Health and Disease. *Cell* **169**, 1000-1011, doi:10.1016/j.cell.2017.05.015 (2017).

19 Baker, D. J. *et al.* Naturally occurring p16(Ink4a)-positive cells shorten healthy lifespan. *Nature* **530**, 184-189, doi:10.1038/nature16932 (2016).

20 Childs, B. G. *et al.* Senescent intimal foam cells are deleterious at all stages of atherosclerosis. *Science* **354**, 472-477, doi:10.1126/science.aaf6659 (2016).

21 Jeon, O. H. *et al.* Local clearance of senescent cells attenuates the development of post-traumatic osteoarthritis and creates a pro-regenerative environment. *Nat Med* **23**, 775-781, doi:10.1038/nm.4324 (2017).
22 Krishnamurthy, J. *et al.* p16INK4a induces an age-dependent decline in islet regenerative potential. *Nature* **443**, 453-457, doi:10.1038/nature05092 (2006).
23 Baker, D. J. *et al.* Clearance of p16Ink4a-positive senescent cells delays ageing-associated disorders. *Nature* **479**, 232-236, doi:10.1038/nature10600 (2011).
24 Scudellari, M. To stay young, kill zombie cells. *Nature* **550**, 448-450, doi:10.1038/550448a (2017).
25 Xu, M. *et al.* Senolytics improve physical function and increase lifespan in old age. *Nat Med*, doi:10.1038/s41591-018-0092-9 (2018).
26 Zhu, Y. *et al.* The Achilles' heel of senescent cells: from transcriptome to senolytic drugs. *Aging Cell* **14**, 644-658, doi:10.1111/acel.12344 (2015).
27 Ng, S. K., Casson, R. J., Burdon, K. P. & Craig, J. E. Chromosome 9p21 primary open-angle glaucoma susceptibility locus: a review. *Clin Experiment Ophthalmol* **42**, 25-32, doi:10.1111/ceo.12234 (2014).
28 Killer, H. E. & Pircher, A. Normal tension glaucoma: review of current understanding and mechanisms of the pathogenesis. *Eye (Lond)* **32**, 924-930, doi:10.1038/s41433-018-0042-2 (2018).
29 Wiggs, J. L. & Pasquale, L. R. Genetics of glaucoma. *Hum Mol Genet* **26**, R21-R27, doi:10.1093/hmg/ddx184 (2017).
30 Burdon, K. P. *et al.* DNA methylation at the 9p21 glaucoma susceptibility locus is associated with normal-tension glaucoma. *Ophthalmic Genet* **39**, 221-227, doi:10.1080/13816810.2017.1413659 (2018).
31 Consortium, E. P. An integrated encyclopedia of DNA elements in the human genome. *Nature* **489**, 57-74, doi:10.1038/nature11247 (2012).
32 Evangelho, K., Mogilevskaya, M., Losada-Barragan, M. & Vargas-Sanchez, J. K. Pathophysiology of primary open-angle glaucoma from a neuroinflammatory and neurotoxicity perspective: a review of the literature. *Int Ophthalmol* **39**, 259-271, doi:10.1007/s10792-017-0795-9 (2019).
33 Justice, J. N. *et al.* Senolytics in idiopathic pulmonary fibrosis: Results from a first-in-human, open-label, pilot study. *EBioMedicine* **40**, 554-563, doi:10.1016/j.ebiom.2018.12.052 (2019).

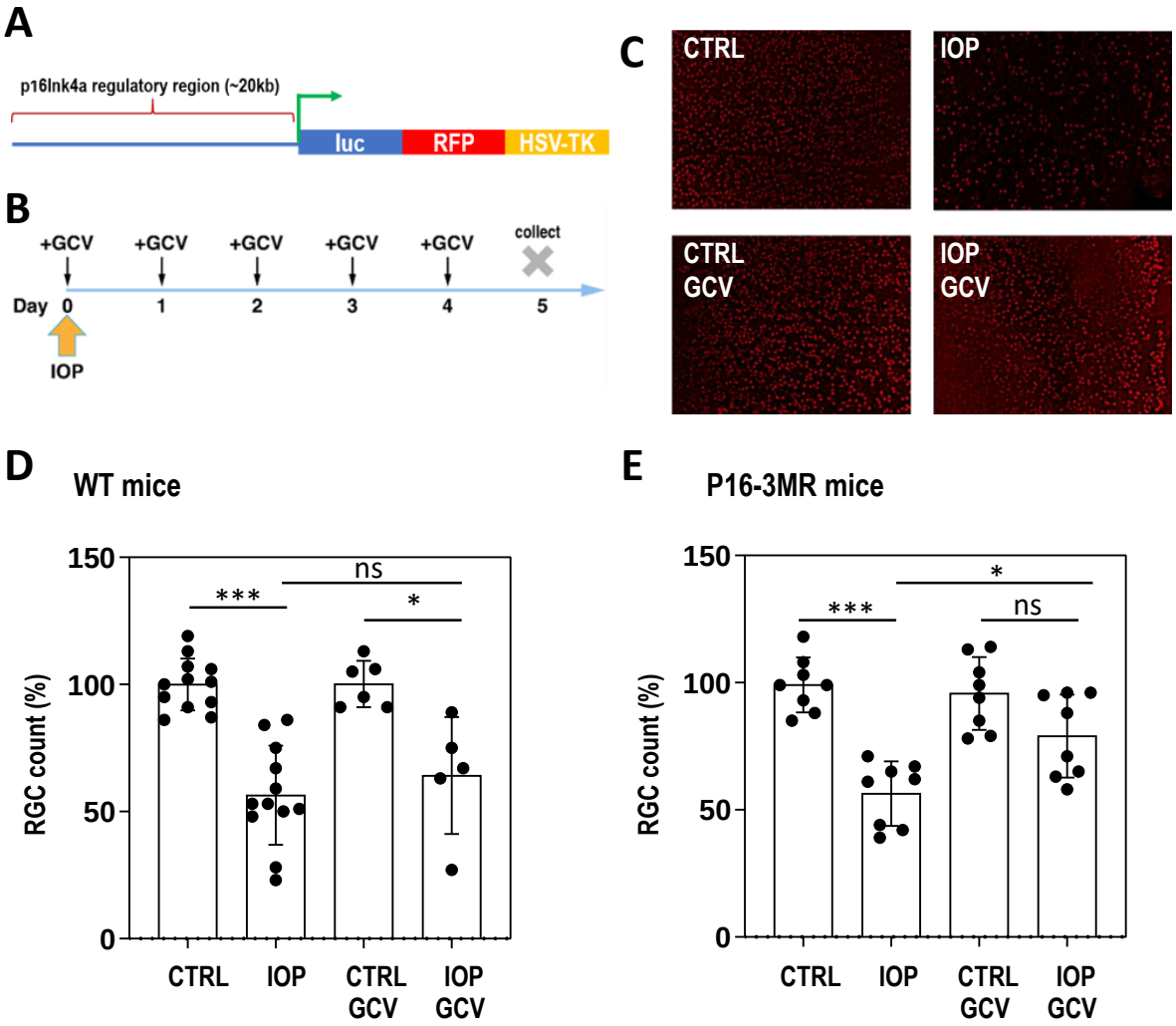

Figure 1. Removal of early senescent cells has neuroprotective effect on RGCs. A. *Schematic representation of the p16-3MR transgene. Triple fusion of luciferase, red fluorescent protein and tyrosine kinase from HSV virus are under control of regulatory region of p16Ink4a gene[8]. **B.** Plan of the experiment. After unilateral IOP elevation mice are daily injected with GCV (25 mg/kg) intraperitoneally. At day 5 VEP is measured and tissue is collected for further experiments. **C.** Representative images of retina flat mount immunohistochemistry at day 5 with anti-Brin3a antibody specifically labelling ~80% of RGC cells. **D.** Quantification of RGC number at day 5 after the treatment of WT animas. N=6 animals in each group **E.** Quantification of RGC number at day 5 after the treatment of p163MR animals. N=6 animals in each group. Statistical test was performed using ANOVA. * p<0.05, ** p<0.01, *** p<0.001, ns – not significant*

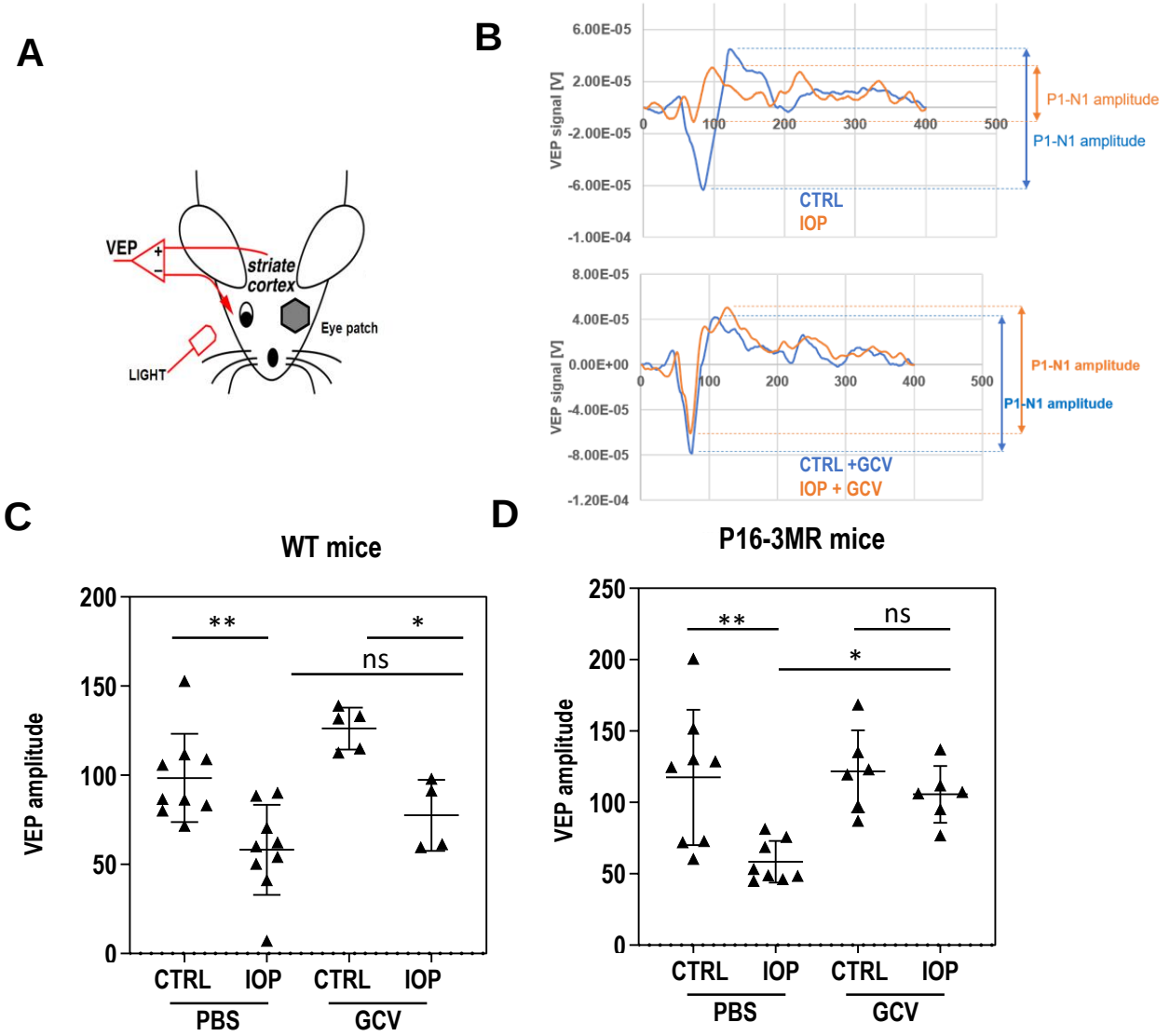

Figure 2. Visual functions are preserved in animals when the early senescent cells were removed. A. *Schematic representation of placement of electrodes for VEP measurements.* ***B****. Example of results VEP experiments. Top: results of VEP response of healthy and IOP treated eyes. Bottom: After GCV injections the VEP response is protected.* ***C.*** *Quantification of VEP responses at day 5 after the treatment of WT animals.* ***D.*** *Quantification of VEP responses at day 5 after the treatment of the p16-3MR animals N=6 animals; t-test, **p<0.01*

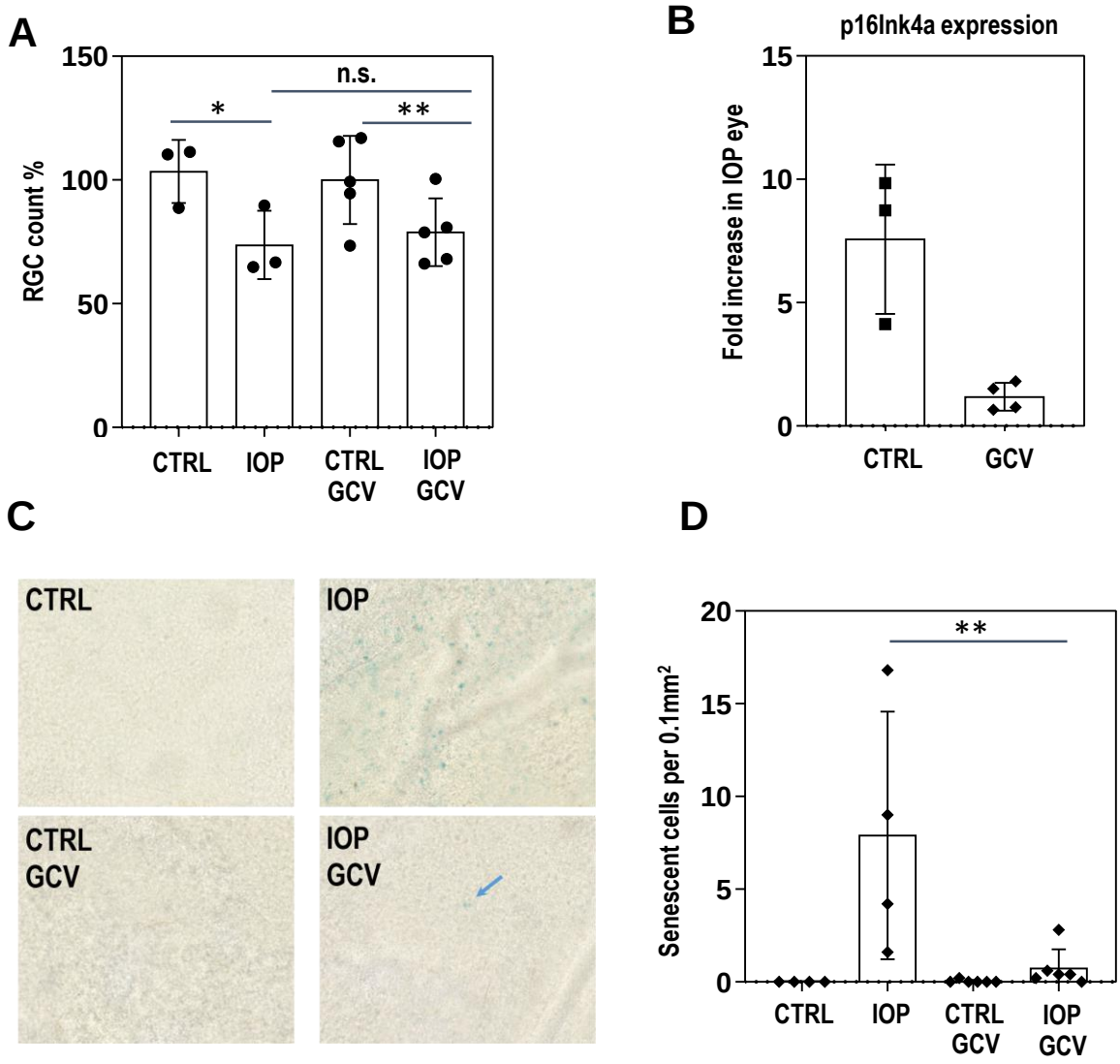

Figure 3. Senescence is lowered upon GCV treatment. A. *At day 3 after IOP only 20% of RGCs is lost compared to the non-treated eye. GCV treatment is removing the same number of cells. n=4 (non-GCV) and n=6 (GCV), ANOVA, *p<0.05, **p<0.01, n.s. – not significant* ***B****. p16Ink4a expression is significantly lower in affected retinas isolated from GCV treated p16-3MR animals at day 3 after IOP elevation. ttest, **p<0.01* ***C****. Number of SA-β-gal positive cells is lowered upon GCV treatment. Blue arrow – remaining senescent cell* ***D****. Quantification of number of senescent cells upon IOP elevation in retinas isolated from mouse treated and non-treated with GCV. n=8 animals; ttest, **p<0.01*

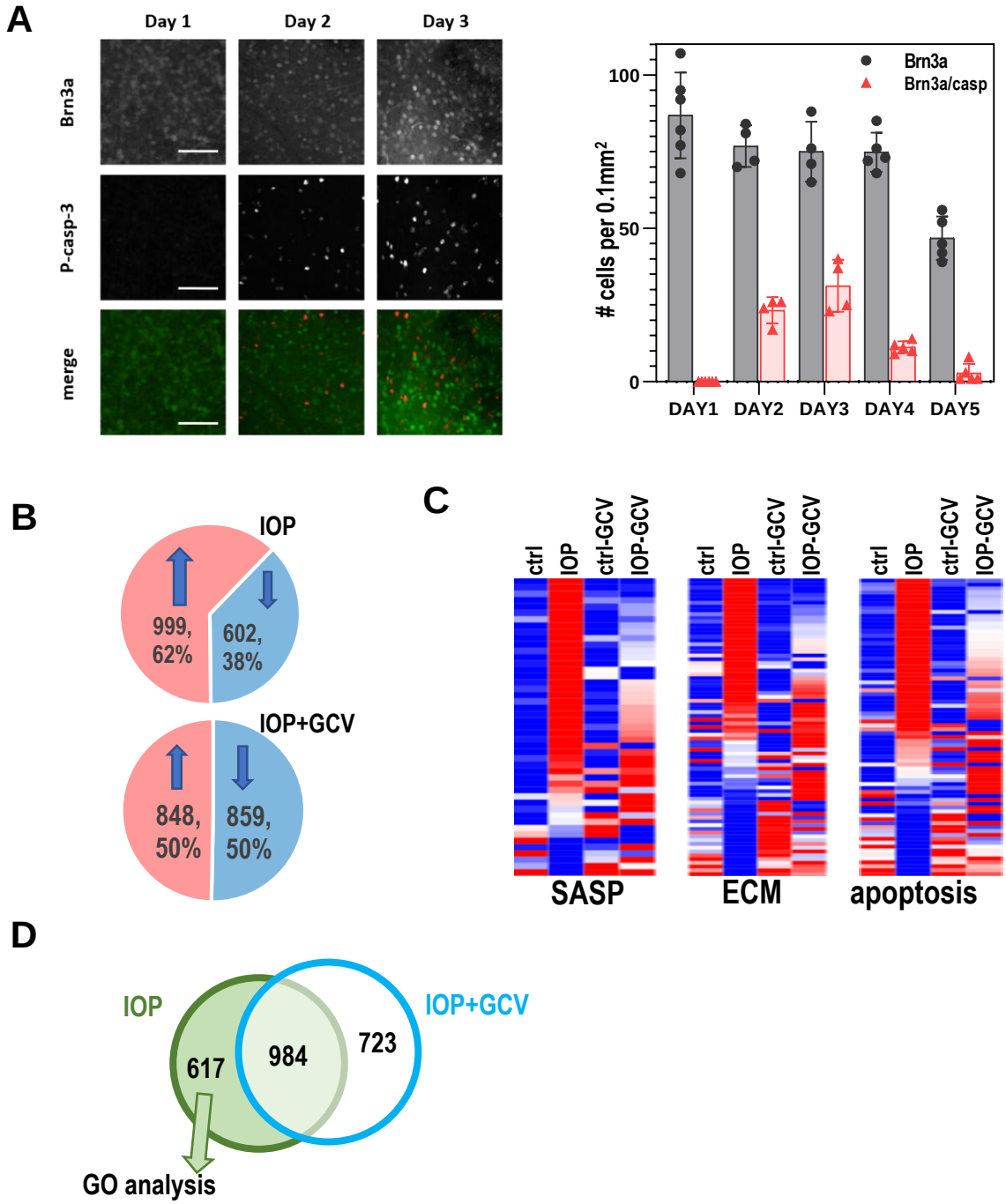

Figure 4. Analysis of pathways affected in IOP treated retinas. A. *Immunohistochemistry of Brn3a and activated caspase show increase of apoptosis at day1, 2 and 3 after IOP treatment. left: quantification of the time-course experiments followed by immunochemistry with Brn3a and activated caspase 3;* ***B,*** *RNA-seq analysis of response to IOP and GCV. Eyes subjected to IOP elevation show significant change in gene expression with more genes upregulated than downregulated. Similar analysis in GCV treated animals shows close to equal distribution of upregulated and downregulated genes* ***C.*** *Heatmap analysis of genes involved in senescence, active oxidative species (ROS), apoptosis, extracellular matrix homeostasis (ECM) and inflammation.* ***D.*** *Venn diagram showing overlap between genes dysregulated upon IOP in GCV treated and untreated retinas. 617 genes specifically dysregulated in IOP only retinas were used for GO analysis.*

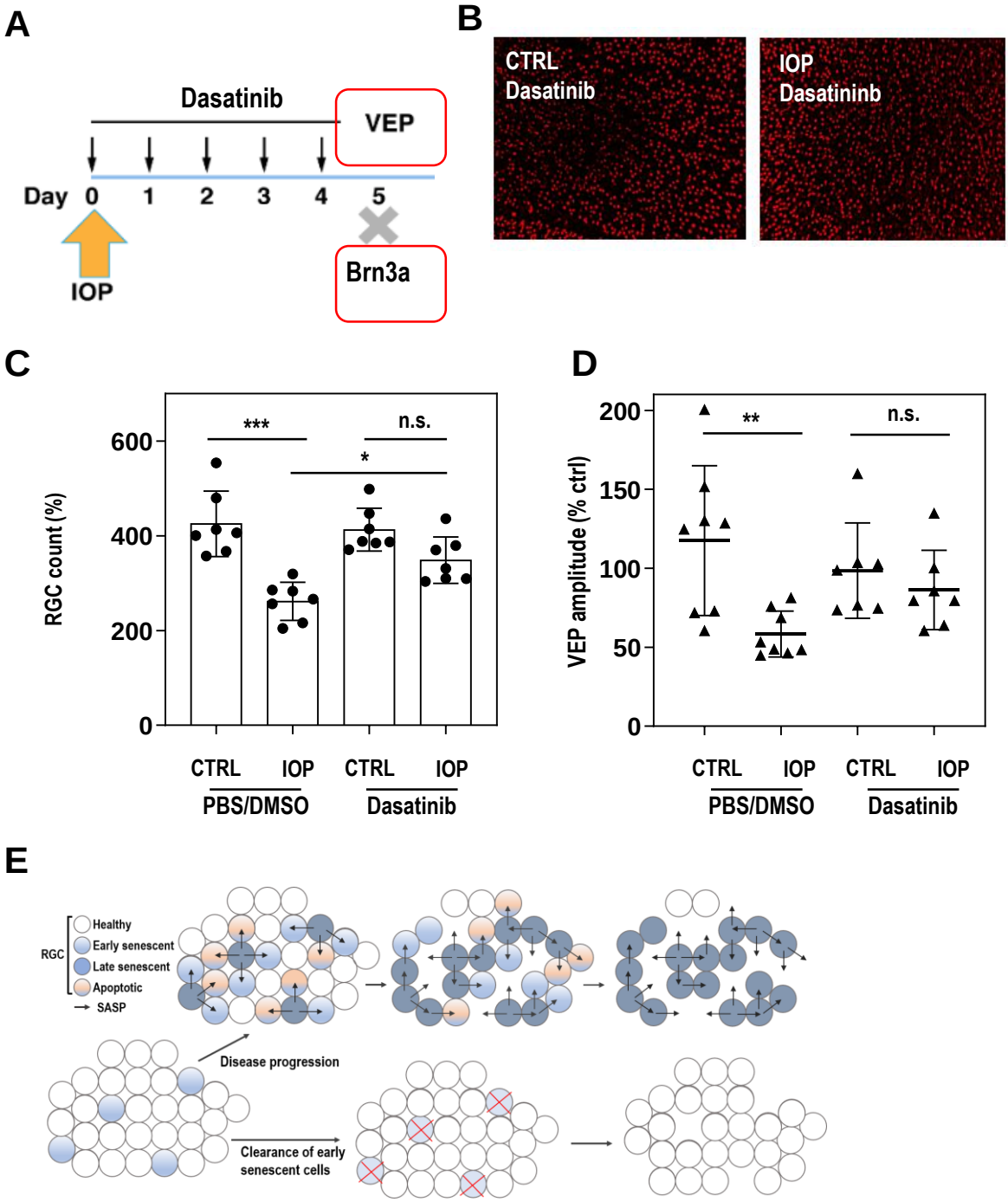

Figure 5. Dasatinib protects retina degeneration. A. *plan of the experiment. After unilateral IOP elevation mice are daily injected with dasatinib (5 mg/kg) intraperitoneally. At day 5 VEP is measured and tissue is collected for further experiments. Immunohistochemistry of Brn3a and activated caspase show increase of apoptosis at day 3 after IOP treatment.* ***B,*** *Retina flat mount immunohistochemistry at day 5 with anti-Brin3a antibody specifically labelling ~80% of RGC cells.* ***C.*** *Quantification of RGC number at day 5 after the treatment of p16-3MR animals with dasatinib. N=6 animals in each group* ***D.*** *Quantification of VEP responses at day 5 after the treatment of p16-3MR animals with dasatinib.* ***E.*** *Model. Top: Upon elevated IOP early damaged cells become senescent and start to express SASP molecules. While disease progresses the SASP molecule induce senescence or apoptosis in neighboring cells. Bottom: When early senescent cells are removed using senolytic drug the neighboring cells are not exposed to detrimental SASPs and the disease progression is significantly slowed down. Remaining cells are healthy.*

A

Kinase perturbation through Enrichr

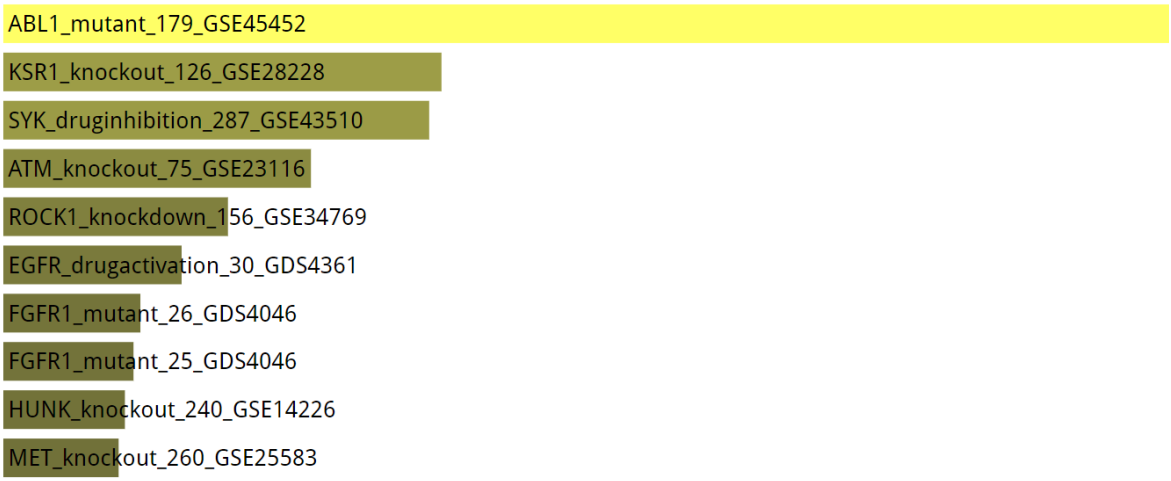

B

Index	Name	P-value	Adjusted p-value	Z-score	Combined score
1	ABL1_mutant_179_GSE45452	6.591e-11	1.879e-8	-1.78	41.66
2	KSR1_knockout_126_GSE28228	0.000007324	0.0006958	-1.71	20.20
3	SYK_druginhibition_287_GSE43510	0.000007324	0.0006958	-1.68	19.84
4	ATM_knockout_75_GSE23116	0.00006225	0.004435	-1.69	16.35
5	ROCK1_knockdown_156_GSE34769	0.0001696	0.009669	-1.60	13.90
6	EGFR_drugactivation_30_GDS4361	0.0004411	0.02095	-1.62	12.54
7	FGFR1_mutant_26_GDS4046	0.001093	0.02595	-1.66	11.32
8	FGFR1_mutant_25_GDS4046	0.001093	0.02595	-1.63	11.12
9	HUNK_knockout_240_GSE14226	0.001093	0.02595	-1.59	10.86
10	MET_knockout_260_GSE25583	0.001093	0.02595	-1.57	10.68

***Supplementary figure 1. Enrichr analysis of* 617 genes altered in PBS conditions by IOP.A.** Kinase perturbation enrichment analysis chart. B. Significance information regarding each pathway.

Analysis Type:	PANTHER Overrepres	
Annotation Version and Release Date:	GO Ontology database	
Analyzed List:	upload_1 (Mus muscu	
Reference List:	Mus musculus (all gen	
Test Type:	FISHER	
Correction:	FDR	
GO biological process complete	Mus musc	upload_1 (
cellular response to interferon-gamma (GO:0071346)	100	17
positive regulation of interleukin-6 production (GO:0032755)	95	14
protein ADP-ribosylation (GO:0006471)	27	8
positive regulation of gliogenesis (GO:0014015)	84	11
lens development in camera-type eye (GO:0002088)	69	10
positive regulation of wound healing (GO:0090303)	55	9
regulation of tyrosine phosphorylation of STAT protein (GO:0042509)	70	10
response to interleukin-1 (GO:0070555)	87	11
cellular response to interleukin-1 (GO:0071347)	72	10
positive regulation of superoxide anion generation (GO:0032930)	20	6
integrin-mediated signaling pathway (GO:0007229)	73	10
respiratory burst (GO:0045730)	13	5
negative regulation of cytokine-mediated signaling pathway (GO:0001960)	48	8
cellular response to cadmium ion (GO:0071276)	23	6
negative regulation of interleukin-6 production (GO:0032715)	49	8
intrinsic apoptotic signaling pathway in response to DNA damage (GO:0008630)	81	10
negative regulation of intracellular transport (GO:0032387)	66	9
negative regulation of response to wounding (GO:1903035)	84	10
lens fiber cell development (GO:0070307)	15	5
negative regulation of response to cytokine stimulus (GO:0060761)	52	8
negative regulation of cell-matrix adhesion (GO:0001953)	38	7
synapse pruning (GO:0098883)	7	4
protein poly-ADP-ribosylation (GO:0070212)	7	4
lens fiber cell differentiation (GO:0070306)	26	6
regulation of macrophage activation (GO:0043030)	53	8
mononuclear cell migration (GO:0071674)	39	7
regulation of homotypic cell-cell adhesion (GO:0034110)	29	6
negative regulation of ERK1 and ERK2 cascade (GO:0070373)	75	9
negative regulation of myeloid leukocyte mediated immunity (GO:0002887)	9	4
I-kappaB kinase/NF-kappaB signaling (GO:0007249)	45	7
iron ion transport (GO:0006826)	45	7
regulation of interleukin-8 production (GO:0032677)	61	8
positive regulation of endothelial cell migration (GO:0010595)	97	10
regulation of calcium-mediated signaling (GO:0050848)	97	10
protein mono-ADP-ribosylation (GO:0140289)	10	4
positive regulation of neuron apoptotic process (GO:0043525)	79	9
protein auto-ADP-ribosylation (GO:0070213)	11	4
regulation of extrinsic apoptotic signaling pathway via death domain receptors (GO:1902(	49	7
protein transport within lipid bilayer (GO:0032594)	49	7
acute inflammatory response (GO:0002526)	66	8

positive regulation of hypersensitivity (GO:0002885)	12	4
interleukin-6-mediated signaling pathway (GO:0070102)	12	4
negative regulation of wound healing (GO:0061045)	68	8
regulation of interleukin-10 production (GO:0032653)	52	7
negative regulation of receptor signaling pathway via JAK-STAT (GO:0046426)	24	5
microglial cell activation (GO:0001774)	24	5
response to lipoprotein particle (GO:0055094)	24	5
regulation of interleukin-12 production (GO:0032655)	53	7
tolerance induction (GO:0002507)	13	4
positive regulation of tyrosine phosphorylation of STAT protein (GO:0042531)	55	7
cellular defense response (GO:0006968)	14	4
cellular extravasation (GO:0045123)	40	6
regulation of cell adhesion mediated by integrin (GO:0033628)	40	6
cellular response to lipoprotein particle stimulus (GO:0071402)	26	5
monoamine transport (GO:0015844)	26	5
response to hydrogen peroxide (GO:0042542)	94	9
positive regulation of membrane invagination (GO:1905155)	15	4
regulation of hypersensitivity (GO:0002883)	15	4
cellular response to low-density lipoprotein particle stimulus (GO:0071404)	15	4
positive regulation of vascular endothelial cell proliferation (GO:1905564)	15	4
regulation of release of sequestered calcium ion into cytosol (GO:0051279)	79	8
positive regulation of interleukin-6 secretion (GO:2000778)	29	5
positive regulation of phosphatidylinositol 3-kinase activity (GO:0043552)	29	5
regulation of type I interferon production (GO:0032479)	80	8
intrinsic apoptotic signaling pathway in response to DNA damage by p53 class mediator ((	31	5
cellular response to amyloid-beta (GO:1904646)	31	5
toll-like receptor signaling pathway (GO:0002224)	47	6
inflammatory response to wounding (GO:0090594)	8	3
positive regulation of cell adhesion mediated by integrin (GO:0033630)	19	4
positive regulation of glial cell differentiation (GO:0045687)	49	6
glial cell activation (GO:0061900)	33	5
positive regulation of lipid kinase activity (GO:0090218)	33	5
regulation of epithelial cell apoptotic process (GO:1904035)	87	8
actin cytoskeleton reorganization (GO:0031532)	68	7
response to axon injury (GO:0048678)	34	5
regulation of oxidative stress-induced neuron intrinsic apoptotic signaling pathway (GO:1!	9	3
amyloid fibril formation (GO:1990000)	9	3
hydrogen peroxide biosynthetic process (GO:0050665)	9	3
response to amyloid-beta (GO:1904645)	35	5
neuroinflammatory response (GO:0150076)	35	5
toll-like receptor 3 signaling pathway (GO:0034138)	9	3
actin-myosin filament sliding (GO:0033275)	9	3
positive regulation of acute inflammatory response (GO:0002675)	35	5

entation Test (Released 20190517)
e Released 2019-02-02
lus)
es in database)

upload_1 (	upload_1 (	upload_1 (	upload_1 (	upload_1 (FDR)
2.48	+	6.85	3.36E-09	2.94E-07
2.36	+	5.94	3.91E-07	2.40E-05
0.67	+	11.95	1.48E-06	7.66E-05
2.08	+	5.28	1.88E-05	7.29E-04
1.71	+	5.84	2.05E-05	7.83E-04
1.36	+	6.6	2.25E-05	8.56E-04
1.74	+	5.76	2.29E-05	8.70E-04
2.16	+	5.1	2.53E-05	9.54E-04
1.79	+	5.6	2.85E-05	1.06E-03
0.5	+	12.1	2.98E-05	1.10E-03
1.81	+	5.52	3.17E-05	1.16E-03
0.32	+	15.51	5.38E-05	1.90E-03
1.19	+	6.72	5.72E-05	2.00E-03
0.57	+	10.52	5.78E-05	2.01E-03
1.22	+	6.58	6.52E-05	2.23E-03
2.01	+	4.98	7.05E-05	2.40E-03
1.64	+	5.5	8.11E-05	2.71E-03
2.08	+	4.8	9.30E-05	3.05E-03
0.37	+	13.44	9.35E-05	3.06E-03
1.29	+	6.2	9.47E-05	3.09E-03
0.94	+	7.43	9.57E-05	3.11E-03
0.17	+	23.04	9.78E-05	3.16E-03
0.17	+	23.04	9.78E-05	3.16E-03
0.64	+	9.3	1.04E-04	3.33E-03
1.31	+	6.09	1.07E-04	3.40E-03
0.97	+	7.24	1.11E-04	3.51E-03
0.72	+	8.34	1.75E-04	5.14E-03
1.86	+	4.84	1.96E-04	5.72E-03
0.22	+	17.92	2.04E-04	5.89E-03
1.12	+	6.27	2.44E-04	6.80E-03
1.12	+	6.27	2.44E-04	6.82E-03
1.51	+	5.29	2.56E-04	7.04E-03
2.41	+	4.16	2.73E-04	7.38E-03
2.41	+	4.16	2.73E-04	7.39E-03
0.25	+	16.13	2.80E-04	7.52E-03
1.96	+	4.59	2.79E-04	7.52E-03
0.27	+	14.66	3.75E-04	9.63E-03
1.22	+	5.76	3.89E-04	9.93E-03
1.22	+	5.76	3.89E-04	9.95E-03
1.64	+	4.89	4.15E-04	1.06E-02

0.3	+	13.44	4.90E-04	1.21E-02
0.3	+	13.44	4.90E-04	1.22E-02
1.69	+	4.74	4.98E-04	1.23E-02
1.29	+	5.43	5.38E-04	1.31E-02
0.6	+	8.4	5.99E-04	1.42E-02
0.6	+	8.4	5.99E-04	1.43E-02
0.6	+	8.4	5.99E-04	1.43E-02
1.31	+	5.33	5.96E-04	1.43E-02
0.32	+	12.41	6.29E-04	1.49E-02
1.36	+	5.13	7.28E-04	1.69E-02
0.35	+	11.52	7.93E-04	1.82E-02
0.99	+	6.05	8.05E-04	1.83E-02
0.99	+	6.05	8.05E-04	1.84E-02
0.64	+	7.75	8.23E-04	1.87E-02
0.64	+	7.75	8.23E-04	1.87E-02
2.33	+	3.86	8.93E-04	1.99E-02
0.37	+	10.75	9.85E-04	2.16E-02
0.37	+	10.75	9.85E-04	2.16E-02
0.37	+	10.75	9.85E-04	2.17E-02
0.37	+	10.75	9.85E-04	2.17E-02
1.96	+	4.08	1.22E-03	2.58E-02
0.72	+	6.95	1.27E-03	2.66E-02
0.72	+	6.95	1.27E-03	2.66E-02
1.98	+	4.03	1.32E-03	2.74E-02
0.77	+	6.5	1.65E-03	3.33E-02
0.77	+	6.5	1.65E-03	3.33E-02
1.17	+	5.15	1.71E-03	3.42E-02
0.2	+	15.12	2.01E-03	3.89E-02
0.47	+	8.49	2.08E-03	3.98E-02
1.22	+	4.94	2.08E-03	3.98E-02
0.82	+	6.11	2.12E-03	3.99E-02
0.82	+	6.11	2.12E-03	4.00E-02
2.16	+	3.71	2.15E-03	4.06E-02
1.69	+	4.15	2.25E-03	4.21E-02
0.84	+	5.93	2.38E-03	4.41E-02
0.22	+	13.44	2.64E-03	4.73E-02
0.22	+	13.44	2.64E-03	4.76E-02
0.22	+	13.44	2.64E-03	4.76E-02
0.87	+	5.76	2.67E-03	4.76E-02
0.87	+	5.76	2.67E-03	4.76E-02
0.22	+	13.44	2.64E-03	4.77E-02
0.22	+	13.44	2.64E-03	4.77E-02
0.87	+	5.76	2.67E-03	4.77E-02

Apoptosis	ECM	SASP
Abl1	Adamts1	Ang5
Actb	Adamts2	Areg
Aifm1	Adamts5	Ccl11
Akt1	Adamts8	Ccl12
Anxa5	Cdh1	Ccl2
Apaf1	Cdh2	Ccl20
Api5	Cdh3	Ccl7
Atf5	Cdh4	Csf2
Bag1	Cntn1	Csf3
Bag3	Col1a1	Ctsb
Bak1	Col2a1	Cxcl11
Bax	Col3a1	Cxcl12
Bcl10	Col4a1	Cxcl13
Bcl2a1a	Col4a2	Egf
Bcl2l10	Col4a3	Egfr
Bcl2l2	Col5a1	Ereg
Bid	Col6a1	Fas
Birc2	Ctgf	Fgf2
Birc3	Ctnna1	Fgf7
Birc5	Ctnna2	Fn1
Bnip2	Ctnnb1	Hgf
Bok	Ecm1	Icam1
Card10	Emilin1	Ifng
Casp1	Entpd1	Igfbp2
Casp12	Fbln1	Igfbp3
Casp14	Fn1	Igfbp4
Casp2	Hapln1	Igfbp5
Casp3	Hc	Igfbp6
Casp4	Icam1	Igfbp7
Casp6	Itga2	Il13
Casp7	Itga3	Il15
Casp8	Itga4	Il1a
Casp9	Itga5	Il1b
Cd40lg	Itgae	Il6
Cd70	Itgal	Il6st
Cflar	Itgam	Il7
Cidea	Itgav	Mip
Cideb	Itgb1	Mmp12
Cradd	Itgb2	Mmp13
Dad1	Itgb3	Mmp14
Dapk1	Itgb4	Mmp1a
Dffa	Lama1	Mmp2
Dffb	Lama2	Mmp3
Diablo	Lama3	Mmp7
Fas	Lamb2	Mmp9
Fasl	Lamb3	Ngf

Gadd45a
Gapdh
Gusb
Hsp90ab1
Igf1r
Il10
Lhx4
Ltbr
Mapk1
Mcl1
Naip1
Naip2
Nfkb1
Nme5
Nod1
Nol3
Polb
Prdx2
Ripk1
Tnfrsf10b
Tnfrsf11b
Tnfrsf1a
Tnfsf10
Tnfsf12
Traf1
Traf2
Trp53
Trp53bp2
Trp63
Trp73
Xiap

Lamc1
Mmp10
Mmp11
Mmp13
Mmp14
Mmp15
Mmp1a
Mmp2
Mmp3
Mmp7
Mmp8
Mmp9
Ncam1
Ncam2
Pecam1
Postn
Sele
Sell
Selp
Sgce
Sparc
Spock1
Spp1
Syt1
Tgfbi
Thbs1
Thbs2
Thbs3
Timp1
Timp2
Timp3
Tnc
Vcam1
Vcan
Vtn

Pigf
Plaur
Serpinb2
Serpine1
Timp1
Timp2
Tnfrsf11b
Tnfrsf1a
Tnfrsf1b
Tnfrsf22